Open Research Online

Citation

URL

https://oro.open.ac.uk/43154/

License

Policy

Versions

Mechanical properties of alginate hydrogels manufactured using external gelation

Georgia Kaklamani,[1,2,3] David Cheneler,[4,5] Liam M Grover,[1] Michael J Adams,[1] James Bowen[1*]

[1] School of Chemical Engineering, The University of Birmingham, Edgbaston, B15 2TT, UK

[2] CNRS, LAAS, N2IS, 7 Avenue du Colonel Roche, F-31400, Toulouse, France

[3] Universite de Toulouse, LAAS, F-31400, Toulouse, France

[4] School of Mechanical Engineering, The University of Birmingham, Edgbaston, B15 2TT, UK

[5] Engineering Department, Lancaster University, Bailrigg, Lancaster, LA1 4YR, UK

[*] Corresponding author: j.bowen.1@bham.ac.uk

Abstract

Alginate hydrogels are commonly used in biomedical applications such as scaffolds for tissue engineering, drug delivery, and as a medium for cell immobilization. Multivalent cations are often employed to create physical crosslinks between carboxyl and hydroxyl moieties on neighbouring polysaccharide chains, creating hydrogels with a range of mechanical properties. This work describes the manufacture and characterisation of sodium alginate hydrogels using the divalent cations Mg^{2+}, Ca^{2+} and Sr^{2+} to promote gelation via non-covalent crosslinks. The gelation time and Young's modulus are characterised as a function of cation and alginate concentrations. The implications of this work towards the use of environmental elasticity to control stem cell differentiation are discussed.

Keywords

Alginate, calcium, cation, hydrogel, indentation, magnesium, modulus, strontium

1

1. Introduction

Hydrogels have been extensively used in biomedical and biomaterials applications, for example as scaffolds for tissue engineering, biosensing and drug delivery technologies, and cell immobilization [1-5]. There is significant interest in their use as matrices for tissue engineering, with both naturally occurring, synthetic, and hybrid materials affording the ability to specify both the mechanical and chemical properties. Cells exhibit the ability to sense the mechanical properties of the environment with which they are in contact [6]. Thus the elastic modulus of polymer hydrogels can influence their migration, development and differentiation [7-8]. Hydrogels also serve as mimics for the extracellular matrix (ECM), which is known to influence the adhesion, geometry and proliferation of cells within their environment [9-11].

Alginate is a naturally occurring polysaccharide derived from brown algae. It is an unbranched block copolymer composed of the two glycan monomers β-D-mannuronic acid (ManA, or M) and α-L-guluronic acid (GulA, or G) [12]. It is non-toxic, biodegradable and can be used to form hydrogels under cytocompatible conditions. Alginate hydrogels have been used in bone and cartilage tissue engineering [13-14], as vehicles for cell delivery, wound dressings, and as matrices to immobilise cells [15-16]. They are commonly formed via ionotropic gelation of dissolved alginate in the presence of multivalent cations such as Mg^{2+}, Ca^{2+}, Sr^{2+} and Ba^{2+} [17-18]. Delivery of the cations into the alginate solution is often performed using an emulsification method, leading to the production of alginate hydrogel beads; this is usually described as internal gelation [19-20]. In contrast, alginate hydrogels can be gelled externally via diffusion of cations from a porous solid support in contact with an alginate solution [21].

The mechanical properties of alginate hydrogels may be tailored through variation of (i) the number and sequence of ManA and GulA monomers, and (ii) the concentration of the polymer in solution. Alginates with high GulA content tend to yield hydrogels with greater mechanical stiffness and strength than those with high ManA content [22]. The elastic modulus depends on the number density of physical crosslinks between chains, conferred by the presence of cations [11]. Alginate hydrogels formed with slower rates of gelation tend to exhibit greater structural homogeneity and therefore larger modulus than those gelled rapidly [23].

The current work characterises the mechanical properties and gelation rate of externally gelled alginate hydrogels, prepared using porous microcellulose sheets as boundary materials. The sheets are separated by a layer of aqueous sodium alginate solution, similar to the methodology previously employed by Hunt *et al.* [21] for the manufacture of 20 mm diameter discs. In contrast, in the work presented here the gelled discs are >100 mm in diameter, prepared using poly(styrene) supports to hold the microcellulose sheets in place. The sheets are saturated with an aqueous solution of divalent cation chloride that diffuses into the alginate solution, the cation acting as a crosslinking agent between the carboxyl groups of the alginate molecules. The Group 2 cations Mg^{2+}, Ca^{2+} and Sr^{2+} are investigated at solution concentrations in the range 1-5 M. The cations Be^{2+} and Ba^{2+} were not investigated because of their toxicity, whilst Ra^{2+} was not investigated because of its radioactivity. The rate of gelation is assessed and the mechanical properties of the resultant hydrogel are measured using indentation. Furthermore, acellular culture media and 3T3 fibroblast-containing culture media are used as a solvent for the sodium alginate and the mechanical properties of these gels are also measured.

External gelation affords the possibility of creating large samples of uniform thickness, with a range of geometries and good reproducibility. The geometry chosen here is a thin disc-like cylinder, formed between parallel platens. The sample exhibits a surface with roughness similar to that of the microcellulose sheet. Further, the samples manufactured in this work are of a geometry suitable for reliably measuring mechanical properties using the spherical indentation technique outlined in §2.5. Samples gelled in this way can also be easily cut to shape for subsequent use. External gelation offers a more rapid gelation than internal gelation, which can typically take up to 48 h. For example the $CaSO_4$/D-glucono-δ-lactone/$CaCO_3$ system reported by Kuo and Ma [23], which requires dispersal of $CaCO_3$ particles within the viscous pre-gelled matrix; a uniform distribution is difficult to achieve, leaving the possibility of local fluctuations in material properties and residual undissolved solid particles within the gel. In contrast, gel beads can be formed rapidly by dripping alginate solution into an aqueous solution of Ca^{2+}, which does not give concern for residual undissolved material. However, this method often results in a polymer concentration gradient within the bead [24].

2. Experimental

2.1 Materials

All chemicals were sourced from Sigma Aldrich (UK) unless otherwise stated. Purities were >99% in all cases. HPLC grade H_2O was employed throughout.
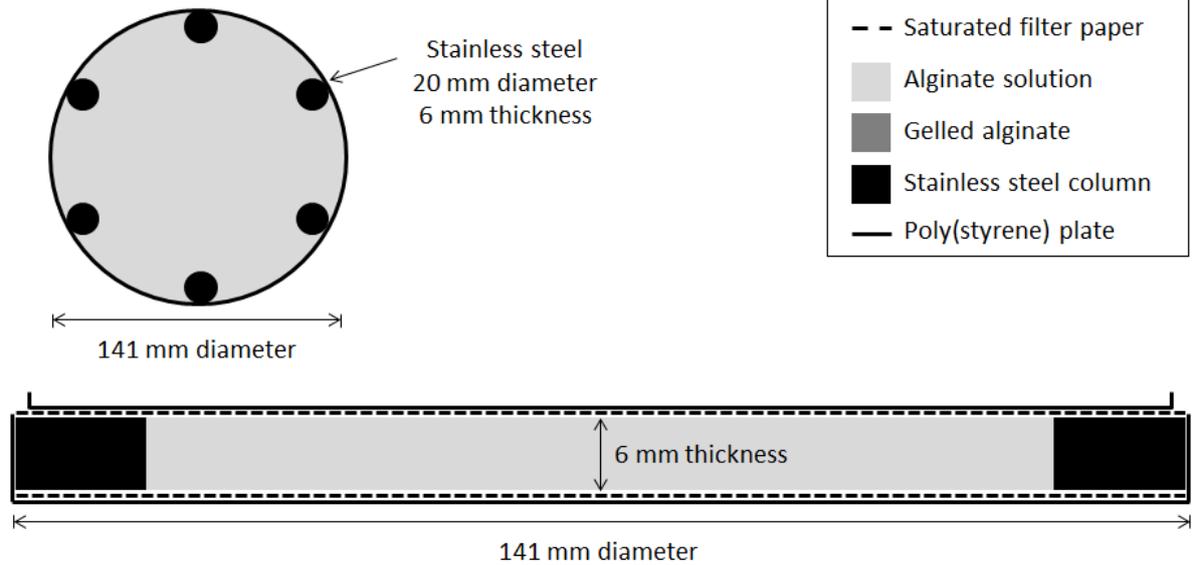

2.2 Hydrogel manufacture

Hydrogels were prepared by an external gelation method in which aqueous sodium alginate solution was poured into a poly(styrene) mould (141.4 mm inside diameter, 9.0 mm inside height, Sterilin, UK) to a liquid height of 6 mm and allowed to gel in the presence of an aqueous solution of cation chloride held at the upper and lower boundaries by porous microcellulose sheets. Prior to the addition of the aqueous sodium alginate solution, stainless steel cylindrical spacers (21 mm diameter, 6 mm height, Longshore Systems Engineering, UK) were placed at 60 ^{o} intervals around the inner edge of the mould in order to support the upper sheet. The volume of aqueous sodium alginate solution required was 81.75 mL. The upper sheet was held in place from above using a poly(styrene) support, filled with water in order to maintain close contact between the upper sheet and the sodium alginate solution as it gelled since some shrinkage was observed at the sample edges. A schematic of this process is shown in Fig. 1.

Sodium alginate powder was dissolved in H_2O under agitated conditions at a temperature of 70 ^{o}C and stirred for a minimum of 2 h using a Stuart US-152 hotplate-stirrer (Appleton Woods, UK). Sodium alginate solutions of concentrations in the range 2.5-5.0% (w/v) were prepared. Aqueous cation chloride solutions of concentrations in the range 1-5 M, where solubility permitted, were created by gradually dissolving the cation chloride powder in water under agitated conditions at room temperature, which in this case was 18 ^{o}C; the dissolution was usually exothermic and hence care was taken when adding powder to the liquid. All solutions were allowed to cool to the room temperature of 18 ^{o}C prior to use. $MgCl_2.6H_2O$, $CaCl_2.2H_2O$, and $SrCl_2.6H_2O$ were used as cation sources. Microcellulose sheets (QL100, Fisherbrand, UK) were trimmed to match the shape of the poly(styrene) mould, and were immersed in aqueous cation chloride solutions for 5 min immediately prior to use. Samples were allowed to gel at 18 ^{o}C for durations of up to 60 min.

For those samples where culture media was used instead of water it was found that attempting to dissolve the sodium alginate directly in the culture media lead to unwanted gelation in the agitated mixing vessel. The successful method involved mixing equal volumes of the culture media and 5.0% (w/v) sodium alginate solution in order to achieve a 2.5% (w/v) sodium alginate solution. Phosphate buffered saline (PBS), Dulbecco's Modified Eagle Medium (DMEM), and DMEM supplemented (S-DMEM) with 10% (v/v) foetal bovine serum (FBS, PAA, Germany) were used as the culture media. For those samples where fibroblasts were suspended in the culture media, cell concentrations of 0.25×10^6, 0.50×10^6, 0.75×10^6, 1.0×10^6 and 2.0×10^6 cells/mL of S-DMEM were prepared. Following mixing equal volumes of fibroblast suspension and 5.0% (w/v) sodium alginate solution, the resulting fibroblast concentrations were in the range $0.125-1.0 \times 10^6$ cells/mL of 2.5% (w/v) sodium alginate solution.

(a) Gelation geometry (aerial and side views)

Stainless steel
20 mm diameter
6 mm thickness

141 mm diameter

Key to figure

- - Saturated filter paper

Alginate solution

Gelled alginate

Stainless steel column

Poly(styrene) plate

6 mm thickness

141 mm diameter

(b) Gelation schematic

(i) Ungelled   (ii) Gelation begins   (iii) Extensive gelation   (iv) Gelled
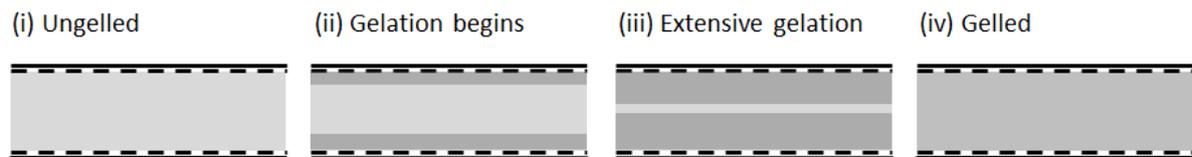
Figure 1. Gelation geometry (a) and gelation schematic (b) showing (i) ungelled alginate solution, (ii)-(iii) progression of the gelation through the alginate solution as the cations diffuse into the alginate solution, generating crosslinks, and (iv) the final, gelled alginate.

2.3 Fibroblast culture

NIH 3T3 fibroblasts were cultured in S-DMEM further supplemented with 2.4% (w/v) L-glutamine, 2.4% (w/v) 4-(2-hydroxyethyl)-1-piperazineethanesulfonic acid (HEPES) buffer and 1% penicillin/streptomycin. Cells were maintained in an incubator (MCO-15AC, Sanyo Electric Co. Ltd., UK) at 37 ^{o}C under an atmosphere of 5% (v/v) CO_2 and 100% relative humidity (RH); media were refreshed every 3 days.

Cells were passaged using 0.25% trypsin-EDTA solution on the 7th day after culture in S-DMEM when they had reached approximately 70% confluency, which was assessed via visual inspection of the cell culture flasks (Iwaki, 75 cm^2 canted neck tissue culture flasks, Sterilin, UK) under a light microscope (Olympus, UK). The sodium alginate solution and cation chloride solutions were autoclaved at 121 ^{o}C for 15 min prior to encapsulation of the fibroblasts and were allowed to cool to 18 ^{o}C before use.

2.4 Live/dead staining

Sections of hydrogel were taken from the centre of samples using a sterilized blade. Extracted sections were immersed in 0.2 µg/mL calcein acetoxymethylester (calcein-AM) for 15 min and 2.5 µg/mL propidium iodide (PI) for 5 min in S-DMEM and incubated at 37 ^{o}C. All

samples were visualized using fluorescence microscopy, employing 490 nm wavelength light for excitation.

2.5 Mechanical testing

The mechanical properties of the hydrogels were measured using spherical indentation. This provided a rapid method for assessing the Young's modulus of samples within 1-2 min of completing the gelation process. Samples were removed from their mould prior to measurement, unless gelation was incomplete; for these samples attempting to extract them from their mould resulted in fracture. Testing was performed using a Z030 mechanical tester (Zwick/Roell, UK) employing a 5 N load cell with a 19.3 mm diameter poly(propylene) sphere (Dejay Distribution, UK) mounted as the indentation probe. Force-displacement data were recorded at a crosshead velocity, *V*, of 0.1 mm/s for indentations of depths <50 µm. Data were fitted to a Hertzian indentation model (Eq. 1) using Matlab (Matlab 2010, Mathworks, US), calculating the Young's modulus for each sample. Each result represents the mean of 15 measurements performed at non-overlapping locations on the sample surface. An example of the measured data and fitted curve are shown in Fig. 3. All measurements were performed at room temperature, in this case 18 $^{\circ}$C.
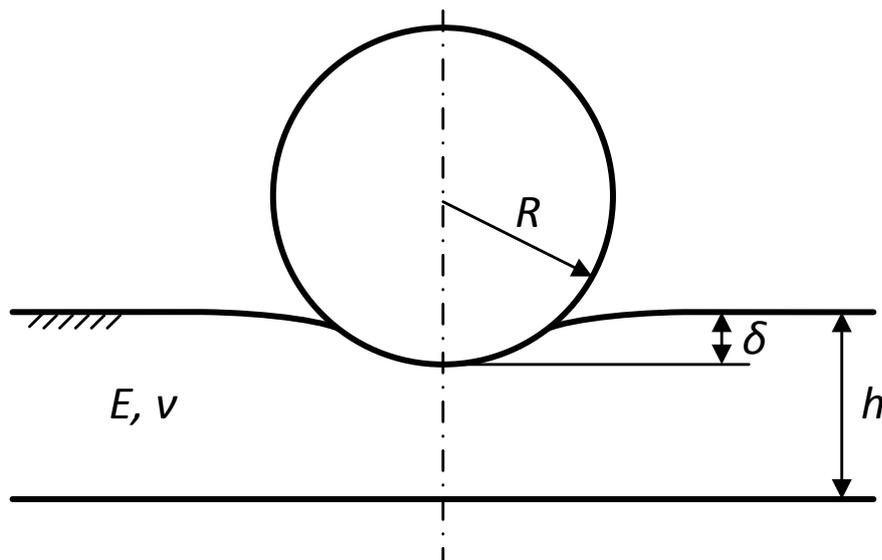

Figure 2. Geometry employed for calculating Young's moduli from measured indentation data

With reference to the indentation schematic shown in Fig. 2, the relationship between indentation depth, δ, and applied force, F, for the case of a rigid sphere being indented into an elastic half-space is given the by Hertz equation [25]:

$$F = \frac{4E}{3(1-v^2)} R^{1/2} \delta^{3/2}$$

(1)

E and v are the Young's modulus and Poisson's ratio of the material respectively and R is the radius of the sphere. However, the sample is not semi-infinite because of the finite thickness compared to the contact radius; this means that the stress field beneath the

6

indentation zone can interact with the effectively rigid substrate, which results in an erroneously large vale of the Young's modulus [26]. Only a few theoretical models exist that take into account the effects of the finite thickness of the material. While most models require extensive numerical computations, Dimitriadis *et al.* [27] derived a simple analytical series solution:

$$F = \frac{4E}{3(1-\nu^2)} R^{1/2} \delta^{3/2} \left[1 - \frac{2\alpha_0}{\pi}\chi + \frac{4\alpha_0^2}{\pi^2}\chi^2 - \frac{8}{\pi^3}\left(\alpha_0^3 + \frac{4\pi^2}{15}\beta_0\right)\chi^3 + \frac{16\alpha_0}{\pi^4}\left(\alpha_0^3 + \frac{3\pi^2}{5}\beta_0\right)\chi^4 \right] \quad (2)$$

where $\chi = \sqrt{R\delta}/h$ and h is the thickness of the sample. The constants α_0 and β_0 are functions of the Poisson's ratio of the material. Dimitriadis *et al.* [27] deduced these constants for both the cases where the sample is either bonded or unbonded to the substrate, which corresponds to stick or slip boundary conditions respectively. The pertinent constants for the stick boundary condition are:

$$\alpha_0 = -\frac{1.2876 - 1.4678\nu + 1.3442\nu^2}{1-\nu}$$

$$\beta_0 = \frac{0.6387 - 1.0277\nu + 1.5164\nu^2}{1-\nu} \quad (3)$$

The pertinent constants for the slip boundary condition are:

$$\alpha_0 = -0.347\frac{3-2\nu}{1-\nu}$$

$$\beta_0 = 0.056\frac{5-2\nu}{1-\nu} \quad (4)$$

Due to the high water content of hydrogels, a nano-film of solvent is expected to form at the interface between the alginate and the platens [28]. The sample is therefore considered not to be bound to the substrate, and as a result there will be slip, but the interface can not be considered frictionless. Hence, the boundary conditions given in Eq. 3 and 4 can be considered upper and lower limits.

Due to the high water content of hydrogels, it is also assumed that the material is incompressible so that $\nu = 0.5$. Therefore, for the stick boundary condition, Eq. 2 can be written as:

$$F = \frac{16E}{9} R^{1/2} \delta^{1/2} \left[1 + 1.133\chi + 1.283\chi^2 + 0.769\chi^3 + 0.0975\chi^4 \right] \quad (5)$$

Similarly, for the slip boundary condition, Eq. 2 can be written as:

$$F = \frac{16E}{9} R^{1/2} \delta^{1/2} \left[1 + 0.884\chi + 0.781\chi^2 + 0.386\chi^3 + 0.0048\chi^4 \right] \quad (6)$$

For the sample thicknesses, indenter geometry, and maximum indentation depth considered in this work, there is a maximum difference in the calculated modulus of < 0.0001% between the two choices of boundary condition. To obtain the Young's modulus, Eq. 6 was fitted to the experimental data using the Levenberg-Marquardt method [29] whereupon:

7

$$\min f(x) = \|F(x)\|_2^2 = \sum_i F_i^2(x) \tag{7}$$

is minimised. Here $\|F(x)\|$ is the residual and $F_i^2(x)$ is the square of the difference between the experimental data and Eq. 6 at each indentation depth. The method was implemented using Matlab's built-in nonlinear least-squares data-fitting function. Fig.3 shows an example of Eq. 6 fitted to indentation data acquired for a 6 mm thickness sample of 5.0% (w/v) sodium alginate gelled using 1 M Ca^{2+} for 60 min.
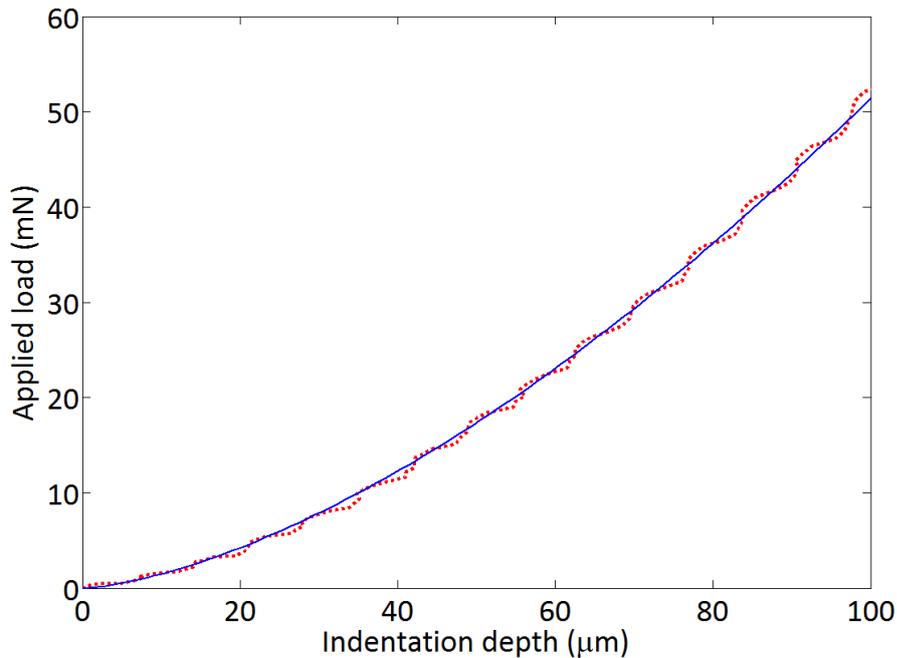

Figure 3. Example indentation data and fitted curve (Eq. 6) for a 6 mm thickness sample of 5.0% (w/v) sodium alginate gelled using 1 M Ca^{2+} for 60 min

3. Results and discussion

3.1 Gelation in the presence of Ca^{2+}

For samples where Ca^{2+} was used as the crosslinking agent, the number of moles of Ca^{2+} retained by the microcellulose sheets used as the upper and lower boundaries was measured as (i) 3.9 mmol for 1 M $CaCl_2$, (ii) 7.9 mmol for 2 M $CaCl_2$, and (iii) 27.3 mmol for 5 M $CaCl_2$. Hence, the total number of moles of Ca^{2+} which could possibly diffuse into the sodium alginate solution are respectively factor of two greater. Fig. 4 shows the Young's moduli of sodium alginate gels formed using solutions of initial concentration in the range 2.5-5.0% (w/v), after a gelation time of 60 min. The results show that the values increase with the number of moles of Ca^{2+} present initially in the microcellulose sheets. They also show that the values increase with increasing sodium alginate concentration, although the moduli of gels formed using initial concentrations of 4.5% (w/v) and 5.0% (w/v) are similar. This suggests that an equilibrium Young's modulus has been achieved for both the 4.5% (w/v) and 5.0% (w/v) formulations. The hydrogels produced by this method exhibit comparable moduli to those produced by internal gelation [23, 30]. The magnitude of the standard errors associated with the mean Young's moduli are in the range ±4-10%. There are four exceptions to this, all for 1 M and 2 M Ca^{2+}, none of which exceed ±20%. The increased variability of the Young's moduli for the 1 M and 2 M Ca^{2+} samples may be indicative of slightly greater heterogeneity. Sodium alginate gels of initial concentration 2.5% (w/v) and 5.0% (w/v), gelled for 60 min using 1, 2 and 5 M Ca^{2+}, were manufactured in triplicate. Statistical analysis revealed no significant difference between the moduli measured for each triplicate of samples.
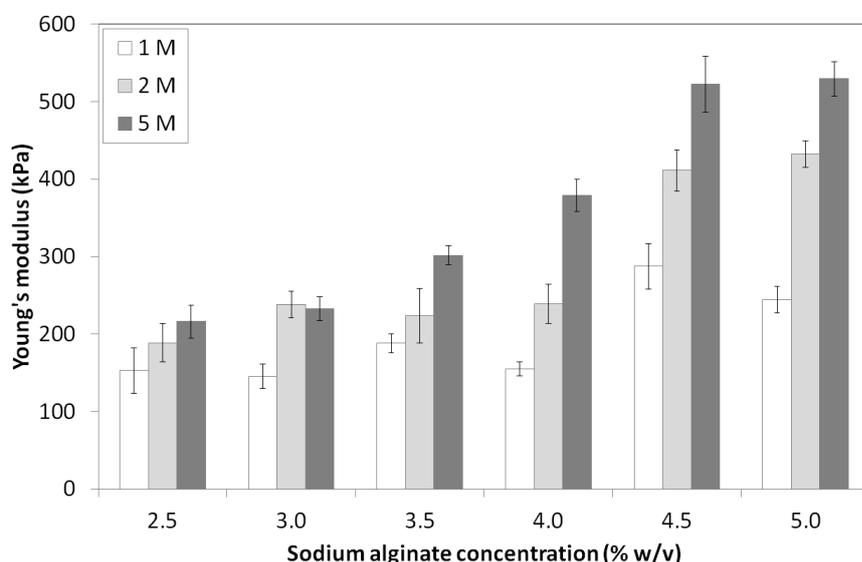

Figure 4. Young's modulus of sodium alginate gels of initial concentration in the range 2.5-5.0% (w/v) gelled for 60 min using 1, 2 and 5 M Ca^{2+}.

The densities of the hydrogels were measured by cutting out a section of lateral dimensions 37.8 mm x 37.8 mm, and measuring the thickness of the slab using a digital caliper (Mitutoyo, UK). The thickness of 5.0% (w/v) hydrogels gelled for 60 min using 1, 2 and 5 M

Ca^{2+} were typically 6.0 ± 0.2 mm, 5.8 ± 0.2 mm, and 5.5 ± 0.2 mm respectively. The hydrogel densities were all within the range 1,050 ± 50 kg/m^3.

Network average mesh sizes, ξ_a, were calculated according to the equation given by Pescosolido *et al.* [31] using Eq. 8, where N_A is Avogadro's constant, and ρ_x is the crosslink density, given by Eq. 9, in which G is the shear modulus of the hydrogel, R_{gas} is the universal gas constant, and T is the absolute temperature.

$$\xi_a = \left(\frac{6}{\pi \, \rho_x N_A} \right)^{1/3} \tag{8}$$

$$\rho_x = \frac{G}{R_{gas}T} \tag{9}$$

The shear modulus of the hydrogel, G, is calculated using the measured Young's modulus, E, and assumed Poisson's ratio ($v = 0.5$) via Eq. 10.

$$G = \frac{E}{2(1+v)} \tag{10}$$

Sodium alginate gels of initial concentration 2.5% (w/v), gelled for 60 min using 1, 2 and 5 M Ca^{2+}, exhibited mesh sizes of 5.3 ± 1.0 nm, 5.0 ± 0.6 nm, and 4.7 ± 0.5 nm respectively. In contrast, sodium alginate gels of initial concentration 5.0% (w/v), gelled for 60 min using 1, 2 and 5 M Ca^{2+}, exhibited mesh sizes of 4.6 ± 0.3 nm, 3.8 ± 0.2 nm, and 3.5 ± 0.2 nm respectively.

Fig. 5 shows the evolution of the calculated Young's modulus of a 5.0% (w/v) sodium alginate/Ca^{2+} mixture as the gelation progresses according to Fig. 1(b). For samples gelled in the presence of 1 M Ca^{2+}, an equilibrium gelation time of 50 min is required. Between 10-40 min, the structure of the sample is approximated by the image shown in Fig. 1(b), whereby solid gelled material surrounds a liquid core. For samples that have not gelled to their centre, the calculated value of the Young's modulus is not an appropriate measure of the sample mechanical properties, but it is nonetheless a useful descriptor for assessing the progress of gelation. For samples gelled in the presence of 2 M Ca^{2+}, the gelation progresses to the centre of the sample within 40 min, while for samples gelled in the presence of 5 M Ca^{2+} the sample has gelled within 20 min. The magnitude of the standard errors associated with the mean Young's moduli are in the range ±6-14%. There are four exceptions to this, all for 1 M and 2 M Ca^{2+}, only one of which exceed ±20% (1 M Ca^{2+}, 20 min).
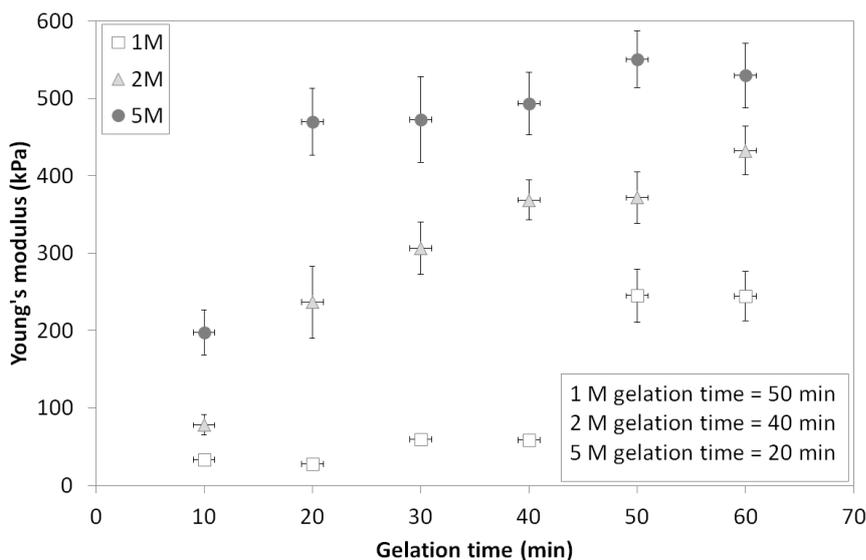
Figure 5. Assessment of gelation time for sodium alginate solutions of initial concentration 5.0% (w/v), gelled using 1, 2 and 5 M Ca^{2+}.

3.2 Gelation in the presence of Mg^{2+} and Sr^{2+}

For samples with an initial concentration of 5.0% (w/v) alginate with Mg^{2+} used as the crosslinking agent, there was no significant gelation after 120 min; attempts were also made using 1, 2, and 5 M Mg^{2+} solutions. Topuz *et al*. [18] reported that Mg^{2+} does promote the gelation of alginate solutions, but the kinetics of gelation are much slower than for Ca^{2+} and the resultant gels exhibited moduli <5 kPa. The samples produced using Mg^{2+} in the work reported here were indistinguishable from the ungelled alginate solution upon performing indentation measurements.

For samples with an initial concentration of 5.0% (w/v) alginate with Sr^{2+} used as the crosslinking agent, gelation was found to occur with similar times to Ca^{2+}. Alginate solutions exposed to 1 M Sr^{2+} gelled within 50-60 min, while alginate solutions exposed to 2 M Sr^{2+} gelled within 40 min. These results are shown in Fig. 6. It was not possible to achieve a 5 M solution of Sr^{2+} due to the limited solubility of $SrCl_2$ in water. The Young's moduli of the alginate/Sr^{2+} gels are significantly less than those of the alginate/Ca^{2+} gels. . The magnitude of the standard errors associated with the mean Young's moduli are in the range ±10-30%. There is one exception to this, 1 M Ca^{2+} for 10 min, which exceeds ±50%. The samples gelled using Sr^{2+} exhibited greater heterogeneity than those gelled using Ca^{2+}, often evidenced by local variation in surface colour, the millimetre scale.

The diameters of the Mg^{2+}, Ca^{2+} and Sr^{2+} ions are 144, 200, and 226 pm respectively [32]. The Mg^{2+} cation exhibits the greatest surface charge density and hence produces the greatest attraction towards the carboxyl and hydroxyl moieties present on the polysaccharide chain. However, the diameter of the cation is sufficiently small that it does not form a strong physical crosslink with the alginate molecules, and hence does not promote gelation; this result is consistent with the findings of Donati *et al*. [33-34] In contrast to the non-gelling alginate/Mg^{2+} system, Ca^{2+} and Sr^{2+} cations have sufficiently large diameters that they promote gelation. The smaller surface charge density of the Sr^{2+} cation

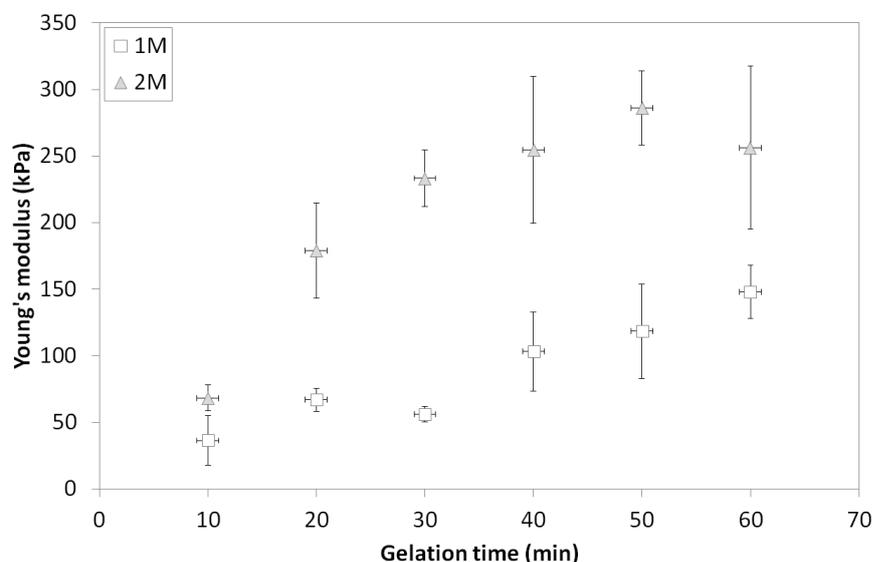compared to the Ca^{2+} cation is proposed as the origin of the smaller values of the Young's modulus.

Figure 6. Assessment of gelation time for sodium alginate solutions of initial concentration 5.0% (w/v), gelled using 1 and 2 M Sr^{2+}.

3.3 Gelation in the presence of cell culture media

A range of acellular samples were produced with an initial alginate concentration of 2.5% (w/v), where cell culture media were used in addition to water, and Ca^{2+} was used as the crosslinking agent at concentrations of 1, 2 and 5 M. The measured Young's moduli for these samples were not significantly different to those samples produced using water only; the results are shown in Fig. 7. In addition, a range of cellular samples were produced where NIH 3T3 fibroblasts were present at concentrations in the range 250-2,000 cells/μL. S-DMEM was used as the cell culture medium, and the samples were crosslinked using 2 M Ca^{2+}. After 60 min gelation time, these samples exhibited moduli in the range 180-210 kPa, i.e. not significantly different to the acellular S-DMEM samples.

These results demonstrate that uniform alginate hydrogels can be manufactured rapidly using a range of cell culture media, in which materials the modulus can be controlled through specifying the concentration of (i) sodium alginate, and (ii) the crosslinking cation.
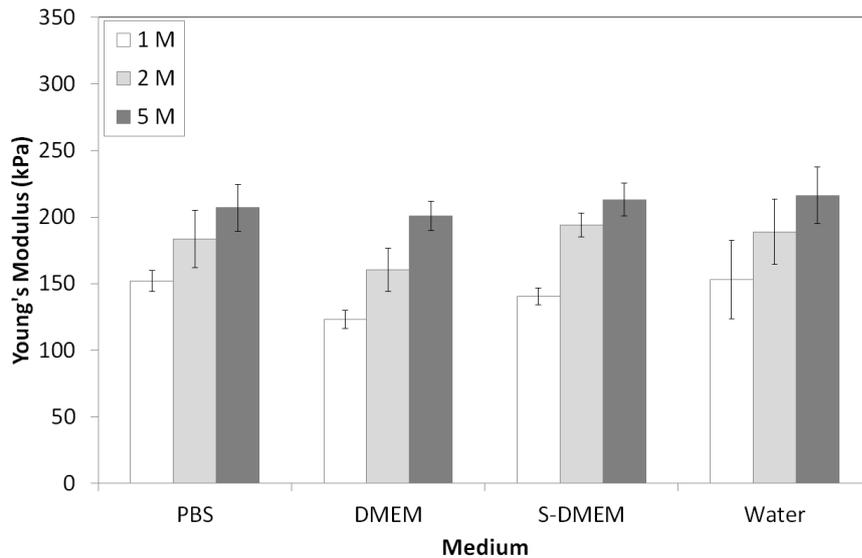
Figure 7. Young's modulus of sodium alginate gels of initial concentration of 2.5% (w/v) gelled in the presence of cell culture media for 60 min using 1, 2 and 5 M Ca^{2+}.

Live/dead staining using calcein-AM and PI showed that fibroblasts encapsulated in sodium alginate gels of initial concentration 2.5% (w/v) and gelled in the presence of cell culture media for 60 min using 1, 2 or 5 M Ca^{2+} were viable for at least 24 h post-gelation. Fig. 8 shows the viability of fibroblasts, evidenced by the abundance of green stain (calcein-AM) and absence of red stain (PI).
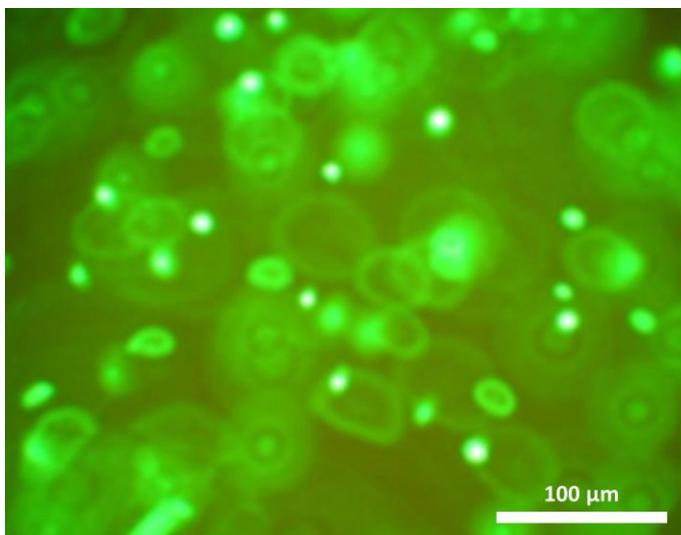

Figure 8. Fibroblast viability assessed using live/dead staining 24 h post-gelation; sodium alginate of initial concentration of 2.5% (w/v) gelled in the presence of cell culture media for 60 min using 5 M Ca^{2+}.

There are a variety of uses for the resultant cellular compatible materials. For example, Engler *et al.* reported that stem cell differentiation can be controlled via careful selection of matrix elasticity [8]. The use of alginate hydrogels such as those reported in this work to direct stem cell differentiation towards osteogenic tissues is an intriguing possibility, and the

subject of future work. The network average mesh size and the degradability or mobility of the physical crosslinks via which the hydrogel is formed are important parameters which must be considered in the context of stem cell differentiation. For example, Khetan *et al*. [35] reported that the differentiation of human mesenchymal stem cells is directed by the generation of degradation-mediated cellular traction.

A further use of hydrogels is in the emerging field of organs-on-chips, an extension of the established lab-on-chip technology. Organ-on-chip seeks to create cell culture microenvironments which mimic organ tissue, organising and culturing living cells within a three-dimensional matrix [36]. Hydrogels including alginate [37] have been used as matrices for this purpose. A greater understanding of the physical properties of these hydrogels, including their mechanical properties, can only be of benefit to researchers.

4. Conclusion

The influence of (i) the divalent cation, (ii) the cation concentration, (iii) the alginate concentration, (iv) the composition of the aqueous medium, has been investigated during the manufacture of sodium alginate hydrogels. Ca^{2+} cations were the most effective of the cations studied for promoting gelation. The Ca^{2+} cation exhibits a diameter sufficiently large to co-ordinate carboxyl and hydroxyl moieties of polysaccharide chains. Sr^{2+} cations are also capable of this, whereas Mg^{2+} cations are too small. Further, the surface charge density of the Ca^{2+} cation affords the gel a network of strong physical crosslinks, whereas the Sr^{2+} cation exhibits a smaller surface charge density, resulting in weaker physical crosslinks and hence lower modulus hydrogels. The hydrogel modulus can be tailored in the approximate range 150-550 kPa via careful selection of the alginate and cation concentration. External gelation using parallel porous microcellulose sheets afforded the reproducible manufacture of samples exhibiting uniform thickness. Furthermore, a range of cell culture media can be employed as the aqueous phase without influencing the mechanical properties of the resultant hydrogel. Future work for studying these materials includes the study of gel fracture following the methodology outlined by Pizzocolo et al. [38] in addition to their flexure strength.

Acknowledgements

References

1. Khademhosseini, A., Langer, R., 2007. Microengineered hydrogels for tissue engineering. Biomaterials 28 (34), 5087-5092.

2. Fedorovich, N.E., Alblas, J., de Wijn, J.R., Hennink, W.E., Verbout, A.J., Dhert, W.J., 2007. Hydrogels as extracellular matrices for skeletal tissue engineering: state-of-the-art and novel application in organ printing. Tissue Eng. 13 (8), 1905-1925.

3. Nicodemus, G.D., Bryant, S.J., 2008. Cell encapsulation in biodegradable hydrogels for tissue engineering applications. Tissue Eng. 14 (2), 149-165.

4. Jen, A.C., Wake, M.C., Mikos, A.G., 1995. Review: hydrogels for cell immobilization. Biotechnol. Bioeng. 50 (4), 357-364.

5. Hoffman, A.S., 2002. Hydrogels for biomedical applications. Adv. Drug. Del. Rev. 54 (1), 3-12.

6. Discher, D.E., Janmey, P., Wand, Y.L., 2005. Tissue cells feel and respond to the stiffness of their substrate. Science 310 (5751), 1139-1143.

7. Peng, X., Huang, J., Deng, H., Xiong, C., Fang, J., 2011. A multi-sphere indentation method to determine Young's modulus of soft polymeric materials based on the Johnson-Kendall-Roberts contact model. Meas. Sci. Technol. 22 (2), 1-6.

8. Engler, A.J., Sen, S., Sweeney, H.L., Discher, D.E., 2006. Matrix elasticity directs stem cell lineage specification. Cell 126 (4), 677-689.

9. Shoichet, M.S., Li, R.H., White, M.L., Winn, S.R., 1996. Stability of hydrogels used in cell encapsulation: an in vitro comparison of alginate and agarose. Biotechnol. Bioeng. 50 (4), 374-381.

10. Brandl, F., Sommer, F., Goepferich, A., 2007. Rational design of hydrogels for tissue engineering: impact of physical factors on cell behaviour. Biomaterials 28 (2), 134-146.

11. Banerjee, A., Arha, M., Choudhary, S., Ashton, R.S., Bhatia, S.R., Schaffer, D.V., Kane, R.S., 2009. The influence of hydrogel modulus on the proliferation and differentiation of encapsulated neural stem cells. Biomaterials 30 (27), 4695-4699.

12. Augst, A.D., Kong, J.K., Mooney, D.J., 2006. Alginate hydrogels as biomaterials. Macromol. Biosci. 6 (8), 623-633.

13. Alsberg, E., Anderson, K.W., Albeiruti, A., Franceschi, R.T., Mooney, D.J., 2001. Cell-interactive alginate hydrogels for bone tissue engineering. J. Dent. Res. 80 (11), 2025-2029.

14. Stevens, M.M., Qanadilo, H.F., Langer, R., Shastri, V.P., 2004. A rapid-curing alginate gel system: utility in periosteum-derived cartilage tissue engineering. Biomaterials 25 (5), 887-894.

15. Mooney, D.J., Lee, K.Y., 2001. Hydrogels for tissue engineering. Chem. Rev. 101 (7), 1869-1878.

16. Drury, J.L., Mooney, D.J., 2003. Hydrogels for tissue engineering: scaffold design variables and applications. Biomaterials 24 (24), 4337-4351.

17. Morch, Y.A., Donati, I., Strand, B.L., Skjåk-Bræk, G., 2006. Effect of Ca^{2+}, Ba^{2+}, and Sr^{2+} on alginate microbeads. Biomacromolecules 7 (5), 1471-1480.

18. Topuz, F., Henke, A., Richtering, W., Groll, J., 2012. Magnesium ions and alginate do form hydrogels: a rheological study. Soft Matter 8 (18), 4877-4881.

19. Chan, L.W., Jin, Y., Heng, P.W.S., 2002. Cross-linking mechanisms of calcium and zinc in production of alginate microspheres. Int. J. Pharm. 242 (1-2), 255-258.

20. Chan, L.W., Lee, H., Heng, P.W.S., 2002. Production of alginate microspheres by internal gelation using an emulsification method. Int. J. Pharm. 242 (1-2), 259-262.

21. Hunt, N.C., Smith, A.M., Gbureck, U., Shelton, R.M., Grover, L.M., 2010. Encapsulation of fibroblasts causes accelerated alginate hydrogel degradation. Acta. Biomater. 6 (9), 3649-3656.

22. Drury, J.L., Dennis, R.G., Mooney, D.J., 2004. The tensile properties of alginate hydrogels. Biomaterials 25 (16), 3187-3199.

23. Kuo, C.K., Ma, P.X., 2001. Ionically crosslinked alginate hydrogels as scaffolds for tissue engineering: Part 1. Structure, gelation rate and mechanical properties. Biomaterials 22 (6), 511-521.

24. Skjåk-Bræk, G., Grasdalen, H., Smidsrød, O., 1989. Inhomogeneous polysaccharide ionic gels. Carbohydrate Polym. 10 (1), 31-54.

25. Hertz H., 1882. Uber die beruhrung fester, elastischer Korper. J. Reine. Angew. Math. 92, 156-171.

26. Domke, J., Radmacher, M., 1998. Measuring the elastic properties of thin polymer films with the atomic force microscope. Langmuir 14 (12), 3320-3325.

27. Dimitriadis, E.K., Horkay, F., Maresca, J., Kachar, B., Chadwick, R.S., 2002. Determination of elastic moduli of thin layers of soft material using the atomic force microscope. Biophys. J. 82 (5), 2798-2810.

28. Masaro, L., Zhu, X.X., 1999. Physical models of diffusion for polymer solutions, gels and solids. Prog. Polym. Sci. 24 (5), 731-775.

29. Marquardt, D., 1963. An algorithm for least-squares estimation of nonlinear parameters. SIAM J. Appl. Math. 11 (2), 431–441.

30. Kong, H.J., Wong, E., Mooney, D.J., 2003. Independent control of rigidity and toughness of polymeric hydrogels. Macromolecules 36 (12), 4582-4588.

31. Pescosolido, L., Feruglio, L.,Farra, R., Fiorentino, S., Colombo, I., Coviello, T., Matricardi, P., Hennink, W.E., Vermonden, T., Grassi, M., 2012. Mesh size distribution determination of interpenetrating polymer network hydrogels. Soft Matter 8 (29), 7708-7715.

32. Marcus, Y., 2009. The standard partial molar volumes of ions in solution. Part 4. Ionic volumes in water at 0-100 ^{o}C. J. Phys. Chem. B 113 (30), 10285-10291.

33. Donati, I., Cesaro, A., Paoletti, S., 2006. Specific interactions versus counterion condensation. 1. Nongelling ions/polyuronate systems. Biomacromolecules 7 (1), 281-287.

34. Donati, I., Asaro, F., Paoletti, S., 2009. Experimental evidence of counterion affinity in alginates: the case of nongelling ion Mg^{2+}. J. Phys. Chem. B 113 (39), 12877-12886.

35. Khetan, S., Guvendiren, M., Legant, W.R., Cohen, D.M., Chen, C.S., Burdick, J.A., 2013. Degradation-mediated cellular traction directs stem cell fate in covalently crosslinked three-dimensional hydrogels. Nature Mater. 12 (5), 458-465.

36. Huh, D., Torisawa, Y., Hamilton, G.A., Kim, H.J., Ingber, D.E., 2012. Microengineered physiological biomimicry: organs-on-chips. Lab Chip 12 (12), 2156-2164.

37. Sung, J.H., Shuler, M.L., 2009. A micro cell culture analog (μCCA) with 3-D hydrogel culture of multiple cell lines to assess metabolism-dependent cytotoxicity of anti-cancer drugs. Lab Chip 9 (10), 1385-1394.

38. Pizzocolo, F., Huyghe, J.M., Ito, K., 2013. Mode I crack propagation in hydrogels is step wise. Eng. Frac. Mech. 97, 72-79.